Structuring Au nanoparticles on two-dimensional MoS_2 nanosheets for electrochemical glucose biosensors

Onur Parlak, Anıl İncel, Lokman Uzun, Anthony P.F. Turner, Ashutosh Tiwari

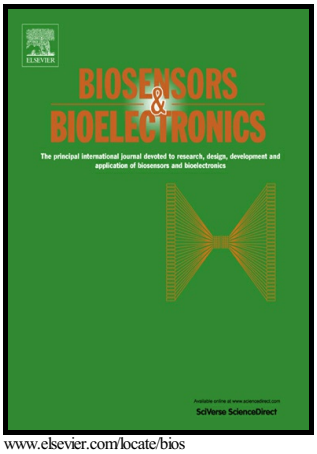

www.elsevier.com/locate/bios

PII: S0956-5663(16)30215-9
DOI: http://dx.doi.org/10.1016/j.bios.2016.03.024
Reference: BIOS8535

To appear in: *Biosensors and Bioelectronic*

Received date: 14 January 2016
Revised date: 6 March 2016
Accepted date: 12 March 2016

Cite this article as: Onur Parlak, Anıl İncel, Lokman Uzun, Anthony P.F. Turner and Ashutosh Tiwari, Structuring Au nanoparticles on two-dimensional MoS nanosheets for electrochemical glucose biosensors, *Biosensors and Bioelectronic* http://dx.doi.org/10.1016/j.bios.2016.03.024

Structuring Au nanoparticles on two-dimensional MoS_2 nanosheets for electrochemical glucose biosensors

Onur Parlak[1,‡], Anıl İncel[1], Lokman Uzun[1,2], Anthony P. F. Turner[1], Ashutosh Tiwari[1,]**

[1]Biosensors and Bioelectronics Centre, IFM, Linköping University, 581 83 Linköping, Sweden
[2]Biochemistry Division, Department of Chemistry, Hacettepe University, Ankara, Turkey

*Corresponding authors.
E-mails: ashutosh.tiwari@liu.se (A. Tiwari), onur.parlak@liu.se (O. Parlak); Tel: (+46)13-28-2395 and Fax: (+46) 13-13-7568.
[‡]Present address: Department of Materials Science and Engineering, Stanford University, 476 Lomita Mall, Stanford, 94305 California, USA

ABSTRACT

Two-dimensional (2D) bioelectronics is an emerging field of research which fuses the advantages of 2D nanomaterials with those of nanobiotechnology. Due to the various physical and chemical properties present in layered counterparts of 2D materials, including high charge density, large surface area, remarkable electron mobility, ready electron transport, sizeable band gaps and ease of hybridisation, they are set to become a versatile tool to fabricate sensitive and selective novel biodevices, which might offer an unique advantages to tackle key energy, medical and environmental issues. Current 2D bioelectronics research is focused on the design of simple-to-use and cheaper biodevices, while improving their selectivity, sensitivity and stability. However, current designs generally suffer from a lack of efficiency, relatively low sensitivity, slow electron transfer kinetics, high background charging current and low current density arising from poor mass transport. Here, we report a nanoparticle-structured MoS_2 nanosheet as an ideal semiconductor interface, which is able to form a homogenous layer on the electrode surface for the assembly of gold nanoparticles. This not only enhances electrocatalytic reactions, but also provides excellent electrochemical

properties such as high faradic-to-capacitive current ratios, high current density and electron mobility, and faster mass transport, due to the dominance of radial diffusion. The MoS_2/Au NPs/GOx bioelectrode exhibits a linear response to glucose from 0.25 to 13.2 mM, with a detection limit of 0.042 µM (S/N = 3) and sensitivity of 13.80 µA/µM/cm^2.

Keywords: Self-assembly, 2D materials, MoS_2 nanosheets, nano-biointerface, biosensor.

1. Introduction

Nanostructuring of metal nanoparticles on electrode surfaces has been beneficial for a variety of biosensor and bioelectronic applications, due to its ability to to enhance surface area and mass transport, facilitate electrocatalysis, control and regulate precise biomolecule-electrode interaction and to regulate the electrode's environment.(Claussen et al. 2009; Claussen et al. 2012; Lin et al. 2005; Parlak et al. 2013; Parlak and Turner 2016; Xuan et al. 2012) From an electrochemical perspective, structuring of conductive nanoparticles on an electrode surface not only enhances electrocatalytic reactions, but also provides excellent electrochemical properties such as high faradic-to-capacitive current ratios, high current density and electron mobility, and faster mass transport by virtue of the dominance of radial diffusion rather than the planar diffucion that occurs in their larger micro/macro electrode counterparts.(Huang et al. 2008; Peng et al. 2009; Zeng et al. 2011) In order to increase the current output and decrease the charging current to reach higher sensitivity, large arrays of nanoparticles on electrode surface have been employed for analytical purposes.(Arrigan 2004; Compton et al. 2008)

The structuring approach has been applied using various size and shaped nanostructures (*e.g.* nanowires, nanotubes and nanoparticles), which have exhibited promising properties such as high sensitivity, faster electron transfer kinetics, low background charging current due to their reduced surface area and high current density arising from enhanced mass

transport.(Cheng et al. 2002; Li et al. 2003; Parlak et al. 2014b, 2015; Yang et al. 2006) There are three common ways to develop nanoparticle based surface structuring: (i) nanoband electrode fabrication; (ii) electrochemical etching; and (iii) electrodeposition of metallic particles. However, the construction of nanostructures, especially by the first two approaches, requires specialised equipment which is relatively complex to use and not cost-effective. Therefore, the third approach is regarded as an easy and practical approach for the construction of nanoparticles on the surface of an electrode. In this method, particles are arranged in an orderly array or randomly dispersed throughout an inert matrix whether by electrodeposition or direct covalent linkage. In the electrodeposition technique, the metal deposition occurs if the potential of an electrode surface immersed in a metallic salt solution becomes negative; therefore, the resulting nanoparticle can be used as a nanoarray for analytical applications.(Lu et al. 2007; Ye et al. 2010) However, in most cases the random construction of nanoparticle arrays throughout the electrode surface limits the possibility of radial diffusion or causes the overlapping of each diffusion layer around each nanoparticle. In addition to this methodology, the synthesis and production of such type of nanoarrays requires special chemical treatments and specific conditions together with additional electrochemical steps. In this study, Au nanoparticles have been structured on two-dimensional molybdenum disulfide (MoS_2) nanosheets in a one-step reaction. The well-dispersed Au nanoparticles were assembled by exploiting the affinity between the coordinated structures of MoS_2 with Au nanoparticles.

In order to obtain successful structuring of gold nanoparticles, layered transition metal dichalcogenides (TMDs) offer an increasingly utility for both fundamental studies and technological applications, due to their unique physical and chemical properties.(Parlak et al. 2014a) Two-dimensional (2D) structures of TMDs are usually denoted MX_2, where M represents a transition metal including Mo, Hf, Ta, W, and X represents the chalcogen such as

S, Se, and Te. Transition metals ranging from Group 4 to Group 10, have different numbers of d-electrons, which fill up the non-bonding d bands to different levels, resulting in varied electronic properties including insulating, semiconducting, metallic and superconducting.(Akinwande et al. 2014) Due to their crystal structures, the physical and chemical properties of 2D TMDs can be effectively tuned through different strategies such as reducing their dimensions, intercalation, heterostructuring, alloying and hybridising with secondary elements. In addition to the chemical composition of 2D TMDs, atomic arrangements also play important roles in determining the material properties.(Xu et al. 2013) The metals and chalcogens are covalently bonded within the molecular layers, which stack together via the weak van der Waals interactions along the *z- axis* to form 3D structures.(Osada and Sasaki 2012) Their recent popularity results not only from their intrinsic material properties, but also on their tunable electronic and catalytic properties.(Chhowalla et al. 2013) Due to the high anisotropy and unique crystal structure, the material properties of 2D TMDs can be modified over a wide regime through different methodologies, including reducing dimensions, intercalation, heterostructuring and hybridising.(Chhowalla et al. 2013; Xu et al. 2013) For example, the band structures are significantly changed, or the carrier densities of 2D TMDs are increased, by intercalation of guest metals, ions or molecules and the electro- and especially bio-electro-chemical properties can be tuned and enhanced by multiple orders of magnitude. Modern technologies and applications require a wide range of high-quality material properties, which are difficult to realise in a single material without modifications. Therefore, 2D TMDs provide an excellent platform for tuning material properties towards desired functions, further attracting a great deal of attention and opening up opportunities for a wide range of applications.(Xu et al. 2013) In addition to all these advanced physical and chemical properties of 2D TMDs, we herein demonstrate the simple formation of a nanostructured electrode interface to overcome the many challenging

limitations for the structuring of nanoparticles. We report a simple approach by direct self-assembling of Au nanoparticles on two-dimensional MoS_2 nanosheets, thus replacing multiple step techniques such as lithography, chemical etching or electrodeposition. We employed MoS_2 as a semiconductor, which is an ideal candidate to form homogenous layer on the electrode surface for the structuring of Au NPs. As an example of a general model enzyme, glucose oxidase (GOx) was assembled on the MoS_2/Au NP hybrid structure. These self-assembled structures were well-dispersed in aqueous solution and were characterised by transmission electron microscopy (TEM), scanning electron microscopy (SEM), atomic force microscopy (AFM), zeta potential and contact angle (CA) measurements.

2. Materials and Methods

2.1. Chemicals

MoS_2 nanosheets (≥99.0% purity, 100-400 nm lateral size, 1-8 monolayers) were obtained from graphene-supermarket (www.graphene-supermarket.com, USA). Gold nanoparticles (Au NPs) (5 nm diameter, 5.5 $x10^{13}$ particles/mL, stabilised suspension in 0.1 M PBS, reactant free), glucose oxidase (GOx) from *Aspergillus niger* (100 U mg^{-1}), potassium dihydrogen phosphate (KH_2PO_4, ≥99.0%), dipotassium hydrogen phosphate (K_2HPO_4, ≥99.0%), potassium chloride (KCl, ≥99.0%), and ferrocene carboxylic acid (97%) were purchased from Sigma-Aldrich (St. Louis, MO, USA) and were used without any further purification. Aqueous solutions were prepared with Milli-Q water (18.2·Ω·cm) obtained by Millipore system (Billerica, MA, USA).

2.2. Preparation of Au NPs-structured MoS_2 nanosheets

MoS_2 nanosheets (10.0 mg) were dispersed in 10 mM PBS solution (pH 7.4, 1 mL) by ultrasonic treatment for 30 min until formation of brownish solution, as shown in the inset Figure 2b. The MoS_2 solution was mixed with gold nanoparticle suspension (100 µL) and the mixture was then incubated at room temperature for 3h to hybridise gold nanoparticles with

MoS_2 nanosheets. The resulting suspension was centrifuged at 5000 rpm for 10 min and rewashed several times with deionised water to remove unassembled particles. Then, MoS_2/Au NPs self-assembled nanosheets were re-dispersed in PBS solution (1 mL) by ultra-sonication around 5 min and mixed with GOx solution in 10 mM PBS at pH 7.4 (1.0 mg/mL). The mixture was kept at 4°C for overnight after 1 min sonication.

2.3. Fabrication of bio-electrode

Before using gold electrode for assembling MoS_2-based structures, they were polished using 1.0, 0.3, and 0.05 micron Buehler alumina slurry on Buehler polishing microcloth (Buehler, Ltd. USA) respectively. The electrodes were then cleaned in the mixture of aqueous ammonia, hydrogen peroxide and water solution (1:1:5 v/v) at 80°C for 10 min and rinsed with excess deionised water. The electrodes were finally electrochemically cleaned in 0.05 M H_2SO_4 solution by cycling between 0.0 V to 1.5 V and allowed to dry at room temperature. Then the dispersions containing MoS_2 based hybrid structures (10 µL) were drop-casted onto the gold electrode surface and then dried at 4°C for overnight. The other modified electrodes were similarly prepared using MoS_2 and MoS_2/GOx nanosheets dispersions.

2.4. Instrumentation

The zeta potential of MoS_2 dispersions was determined using a Nano ZS dynamic light-scattering (DLS) - Zeta potential instrument (Malvern Instruments, Worcestershire, UK). Transmission electron microscopy (TEM) was performed using a G^2 Spirit/Biotwin (FEI-Technai, Hillsboro, OR, USA) with a working voltage of 120 kV. All the voltammetric and amperometric measurements were carried out with Ivium Stat.XR electrochemical analyser (Eindhoven, The Netherlands). The three-electrode cell with gold plate working electrode having 0.5 cm^2 surface area and platinum wire auxiliary, and Ag/AgCl (3 M KCl) reference electrodes were used for the voltammetry and amperometry measurements.

3. Results and discussion

Scheme 1 demonstrates the general process for the structuring of Au NPs on MoS_2 nanosheets and assembly of the enzyme for detection of glucose in the presence of the mediator, ferrocene carboxylic acid, in solution. The synthesis strategy is to initially obtain self-assembled MoS_2/Au NP hybrid nanosheets on a gold electrode surface. This is the crucial step to achieve a free-standing and stable dispersion for further enzyme assembly. The further step involves the conjugation of the enzyme with MoS_2/Au NP nanosheets to acheive an orderly self-assembled bio-interface.

3.1. Preparation of Au NPs-structured MoS_2 nanosheets

Figure 1 and Figure S1-2 (Supporting Information) show the TEM images of MoS_2 nanosheets before (a-b) and after (c-d) assembly of the colloidal Au NPs. The panel a-b in Figure 1 illustrates wrinkled and folded sheet morphologies, which may originate from the reaction sites involved in the oxidation and reduction processes, respectively. Although the MoS_2 nanosheets are very thin, a stack of few layers is clearly visible (Figure 1a). Figure 1c-d shows assembled MoS_2 monolayers with high surface coverage. Here, the images also show that Au NPs selectively prefer the MoS_2 surface due to the surface affinity between MoS_2 coordinated structures and Au NPs.

We prepared ordered MoS_2/Au NPs/enzyme hybrid structures through spontaneous self-assembly mainly via electrostatic interactions. The surface charge of neat MoS_2 nanosheets, measured at different pH values, indicated that the MoS_2 nanosheet was highly negatively charged over a wide pH range. This varied between -57 mV and -21 mV over a pH range from 2 to 11, respectively. **Figure 2**a illustrates that the MoS_2 nanosheets carry a high negative charge on the surface (-30.0 ± 2.5 mV) when the zeta potential measurements are performed under physiological conditions (pH 7.4). In addition to the MoS_2, the surface charge of the gold nanoparticle colloid was measured at different pHs (2-12). The results reveal that the gold nanoparticles were highly negatively charged at low pH (2-6). However,

the surface charge starts to turn positive above pH 7.4 and reached +7 mV (pH 8) and finally +13 mV (pH 12).(Parlak et al. 2014a) The positive charge provided a strong interaction with Au NPs and facilitated a high loading. However, a decay was observed while Au NPs were assembled on the MoS_2 surface and the particles were randomly distributed; the negative value of the surface zeta potential decreased slightly to -23.0 ± 3.0 mV due to the insertion of Au NPs with higher positive surface charge. After enzyme immobilisation on the MoS_2/Au NP assembled nanosheets, the value decreased to -9.0 ± 3.0 mV at pH 7.4. The surface wettability also decreased during modification process. The initial water contact angle of 70° decreased to 58° and then 46°, after assembly of the Au NPs and enzyme immobilisation, respectively (Figure 2b). These results demonstrate that electrostatic attraction is the dominant driving force throughout the modification process and could be controlled by varying the pH of the reaction medium.

3.2. Electrochemical characterisations of modified electrodes

The interfacial electrochemical properties of all modified electrodes were characterised by cyclic voltammetry (CV), electrochemical impedance (EIS) in 0.1 M PBS solutions containing 1 mM ferrocene carboxylic acid and 0.1 M KCl (Figure 3-5 and Figure S4). The CV responses of all MoS_2 nanosheet-based structures displayed a classical sigmoidal shape with narrow peak-to-peak potential separations, indicating fast electron transfer kinetics. When the electrode surface was modified with the MoS_2-Au NPs assembly on nanosheets, the peak current of ferrocene carboxylic acid increased relative to the MoS_2 modified nanosheets alone, which indicates that structuring of the nanoparticle creates a higher electroactive surface area and provides a more conductive interlayer for the electron transfer (**Figure 3**). The electroactive surface area (*A*) for the modified electrodes was calculated based on Randles–Sevcik equation, which assumes mass transport occurred only by diffusion:(Lu et al. 2008)

$$I_p = 2.69 \times 10^5 A D^{1/2} n^{3/2} \gamma^{1/2} C \quad (1)$$

where *n* is the number of electron involving in the redox process, *D* is the diffusion coefficient of the molecule (6.70 x 10^{-6} cm^2/s), *C* is the concentration of the probe molecule in the solution (mol/cm^3) and γ is the scan rate ($V \cdot s^{-1}$). The surface area for MoS_2 and MoS_2/Au NPs nanosheets was found to be 0.42 cm^2 and 0.65 cm^2, respectively. Thus, the structuring of Au NPs caused a 1.5-fold increase in the effective surface area of the nanosheets.

The charge transfer properties of electrodes modified by different MoS_2 based self-assembled nanostructures were further characterised by electrochemical impedance spectroscopy (**Figure 4**a-b). The Randles circuit was chosen to fit the impedance outputs.(Chang and Park 2006) The Nyquist plots of spectra, which contain semi-circular and linear portions, indicate both limited electron transfer (semi-circular portion) and diffusion process (linear portion) occurred simultaneously. The charge transfer resistance (R_{CT}) at the electrode surface can be quantified based on the diameter of the semi-circular part of the plot. According to calculation, the R_{CT} of MoS_2 and MoS_2/Au NP nanosheet-modified electrode were 0.46 kΩ and 0.66 kΩ, respectively, which were significantly higher than for the bare gold electrode (0.06 kΩ). Thus, after immobilisation of the enzyme on the surface of MoS_2/Au NP nanosheets, a slight inhibition of electron transfer of the redox couple was observed (0.89 kΩ), due presumably to the insulating effect of organic/biolayers.

Moreover, we investigated the electrocatalytic oxidation of glucose at the MoS_2, MoS_2/GOx and MoS_2/Au NP/GOx nanosheet-electrodes by amperometric measurements (**Figure 5**a) for the successive additions of glucose at an applied voltage of + 350 mV (vs. SCE) in 1 mM of ferrocene carboxylic acid and 0.1 M PBS (pH 7.4). MoS_2-modified nanosheet electrodes showed no electrocatalytic response to the entire range of additions of glucose, and this electrode could did yield any detectable current increase. In contrast, the MoS_2/Au NP/GOx and MoS_2/GOx nanosheet-electrodes displayed a rapid and sensitive

response to the addition of glucose, and a steady-state current was obtained within 3 and 5 s, respectively. The fast response may be attributed to the fast diffusion in the open three-dimensional structure of the assembly and the perfect surface wettability that allows substrate molecules to easy and rapid diffusion through electrode surface. Furthermore, well-defined current responses proportional to glucose concentrations were observed with both electrode surfaces.

A calibration curve of the electrocatalytic currents generated in response to glucose concentration is presented in Figure 5b. The catalytic current displays a linear relationship to glucose concentration in the range from 0.25 to 7.0 mM for MoS_2/GOx nanosheets. However, the dynamic range was greatly improved for MoS_2/Au NP/GOx assembled nanosheets (0.25 mM to 13.2 mM). The sensitivity and detection limit of MoS_2/Au NP/GOx electrode were 13.8 μA/μM/cm^2 and 0.042 μM (S/N=3), respectively (Table S2, Supporting Information). Accordingly, the MoS_2/Au NPs/GOx nanosheet-electrode provided good catalytic performance for the detection of glucose over a relatively wide linear range, high sensitivity and a low detection limit. Such high catalytic properties of the enzyme electrode is ascribed to the open structures of the MoS_2/Au NP/GOx assembly, the large surface area of MoS_2 nanosheets for enzyme immobilisation, fast mass transport due to the large interlayer distance of ordered structure, bio- and water-compatibility of MoS_2 and the synergistic catalytic effect of MoS_2/Au NPs.

4. Conclusion

In conclusion, we have demonstrated the fabrication of an electrochemical biosensor based on MoS_2 nanosheets and the effect of nanostructuring of metal particles using a simple, inexpensive and high order two-dimensional biosystem, which is highly sensitive, selective and stable. The results have shown that bioelectrocatalytic reactions can be controlled and regulated by modifying the nanointerface. The material we have designed could potentially

provide significant improvements in biocatalysis and nanotechnology by exploiting this novel biocatalytic interface with a variety of redox enzymes.

Acknowledgements

The authors wish to acknowledge the Swedish Research Council (VR-2011-6058357) for the generous financial support to carry out this research.

Appendix A. Supporting information

Supplementary data associated with this article can be found in the online version.

References

Akinwande, D., Petrone, N., Hone, J., 2014. Two-dimensional flexible nanoelectronics. Nature Communications 5 (5678), 1-12.
Arrigan, D.W.M., 2004. Analyst 129 (12), 1157-1165.
Chang, B.Y., Park, S.M., 2006. Analytical Chemistry 78 (4), 1052-1060.
Cheng, W.L., Dong, S.J., Wang, E.K., 2002. Langmuir 18 (25), 9947-9952.
Chhowalla, M., Shin, H.S., Eda, G., Li, L.-J., Loh, K.P., Zhang, H., 2013. Nature Chemistry 5 (4), 263-275.
Claussen, J.C., Franklin, A.D., ul Haque, A., Porterfield, D.M., Fisher, T.S., 2009. ACS Nano 3 (1), 37-44.
Claussen, J.C., Kumar, A., Jaroch, D.B., Khawaja, M.H., Hibbard, A.B., Porterfield, D.M., Fisher, T.S., 2012. Advanced Functional Materials 22 (16), 3399-3405.
Compton, R.G., Wildgoose, G.G., Rees, N.V., Streeter, I., Baron, R., 2008. Chemical Physics Letters 459 (1-6), 1-17.
Huang, T., Nallathamby, P.D., Xu, X.-H.N., 2008. Journal of the American Chemical Society 130 (50), 17095-17105.
Li, J., Ng, H.T., Cassell, A., Fan, W., Chen, H., Ye, Q., Koehne, J., Han, J., Meyyappan, M., 2003. Nano Letters 3 (5), 597-602.
Lin, Y.H., Cui, X.L., Yen, C., Wai, C.M., 2005. Journal of Physical Chemistry B 109 (30), 14410-14415.
Lu, J., Do, I., Drzal, L.T., Worden, R.M., Lee, I., 2008. ACS Nano 2 (9), 1825-1832.
Lu, Y., Yang, M., Qu, F., Shen, G., Yu, R., 2007. Bioelectrochemistry 71 (2), 211-216.
Osada, M., Sasaki, T., 2012. Advanced Materials 24 (2), 210-228.
Parlak, O., Seshadri, P., Lundstrom, I., Turner, A.P.F., Tiwari, A., 2014a. Advanced Materials Interfaces 1 (6).
Parlak, O., Tiwari, A., Turner, A.P.F., Tiwari, A., 2013. Biosensors & Bioelectronics 49, 53-62.
Parlak, O., Turner, A.P.F., 2016. Switchable bioelectronics. Biosensors & Bioelectronics 76, 251-265.
Parlak, O., Turner, A.P.F., Tiwari, A., 2014b. Advanced Materials 26 (3), 482-486.
Parlak, O., Turner, A.P.F., Tiwari, A., 2015. Journal of Materials Chemistry B 3 (37), 7434-7439.
Peng, H.-I., Strohsahl, C.M., Leach, K.E., Krauss, T.D., Miller, B.L., 2009. ACS Nano 3 (8), 2265-2273.
Xu, M., Liang, T., Shi, M., Chen, H., 2013. Chemical Reviews 113 (5), 3766-3798.

Xuan, J., Jia, X.-d., Jiang, L.-P., Abdel-Halim, E.S., Zhu, J.-J., 2012.. Bioelectrochemistry 84, 32-37.
Yang, M., Qu, F., Lu, Y., He, Y., Shen, G., Yu, R., 2006. Biomaterials 27 (35), 5944-5950.
Ye, W., Yan, J., Ye, Q., Zhou, F., 2010. Journal of Physical Chemistry C 114 (37), 15617-15624.
Zeng, Q., Cheng, J.-S., Liu, X.-F., Bai, H.-T., Jiang, J.-H., 2011. Biosensors & Bioelectronics 26 (8), 3456-3463.

Scheme 1. Schematic representations of Au nanoparticle-structuring on a MoS_2 interface and mediated electron transfer process in the MoS_2/Au NPs/GOx hybrid structure on the gold electrode.

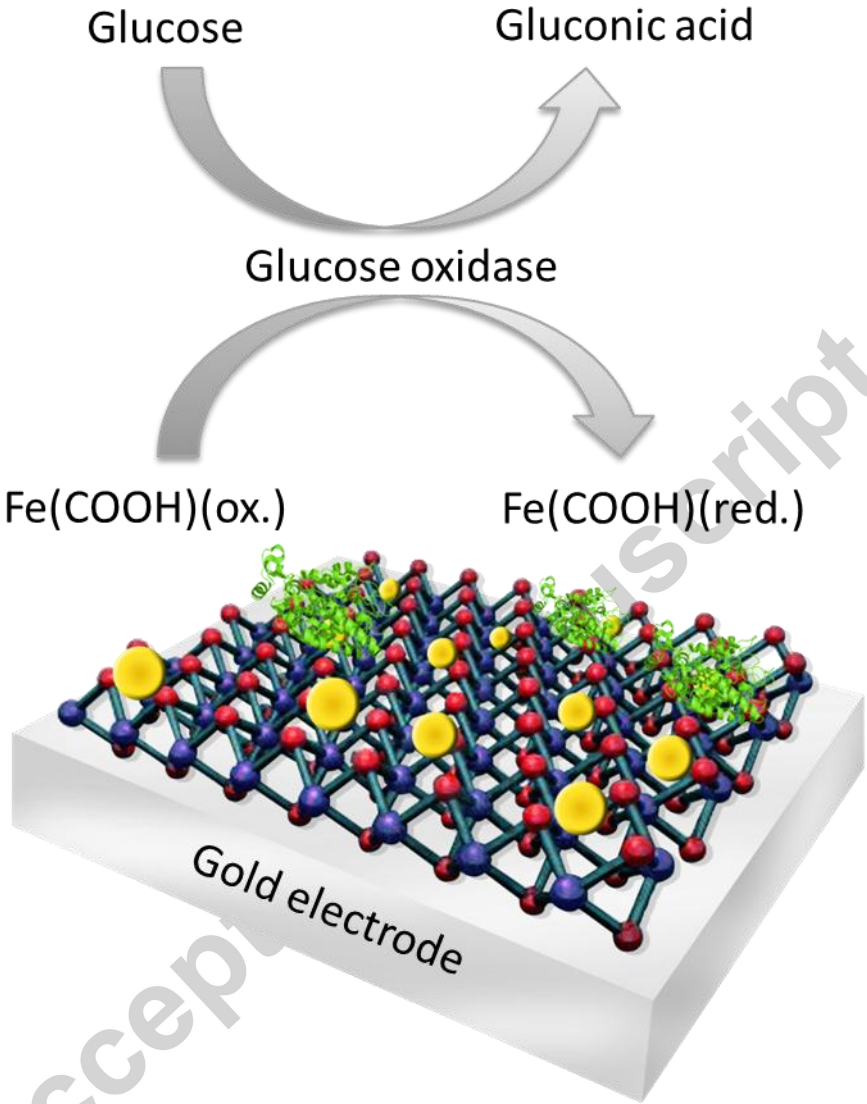

Figure 1. TEM images of MoS_2 nanosheets at (a) low, and (b) high magnification, and Au NPs structured MoS_2 nanosheets at (c) low and (d) high magnification.

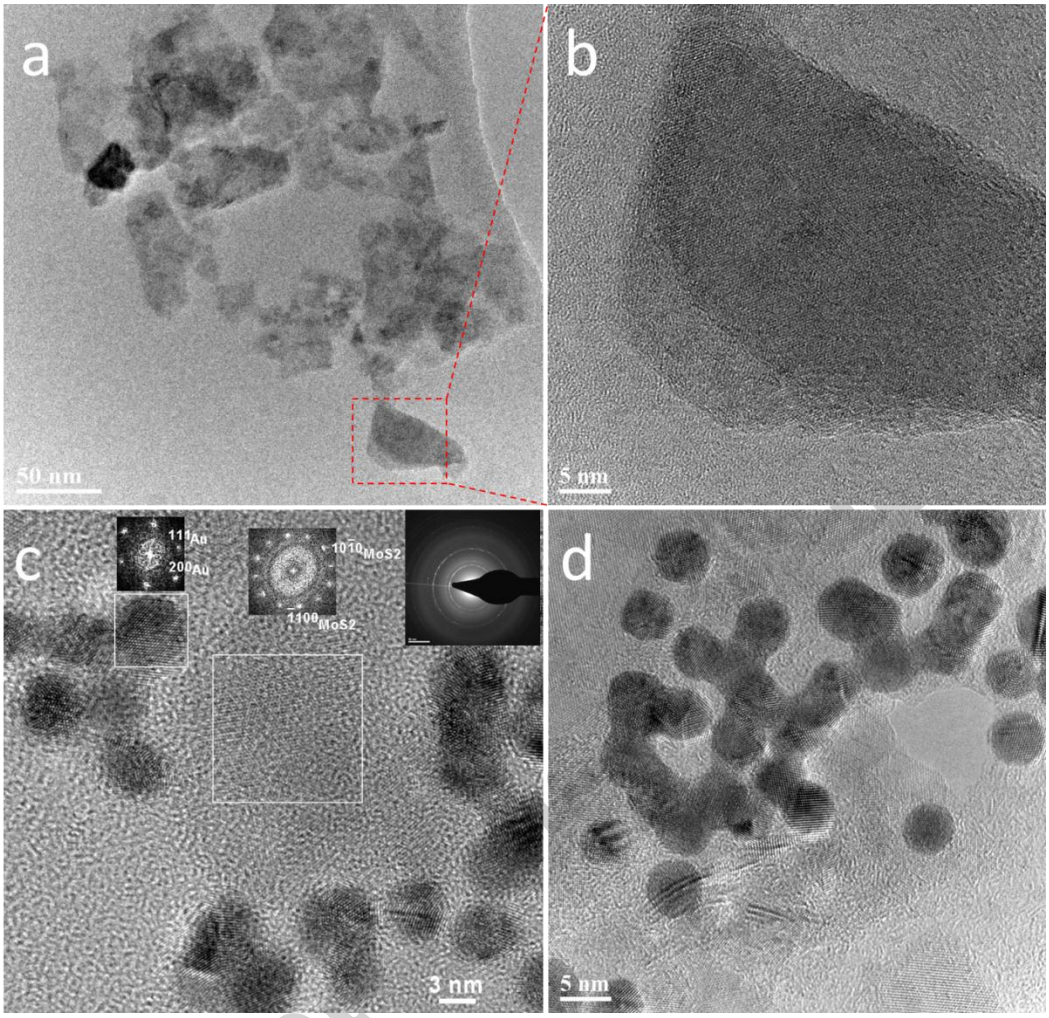

Figure 2. The zeta potential (a) and water contact angle (b) of MoS_2, Mo_2/Au NPs and MoS_2/Au NPs/GOx nanosheets. The inset in b represents powder and dispersion forms of MoS_2 nanosheets.

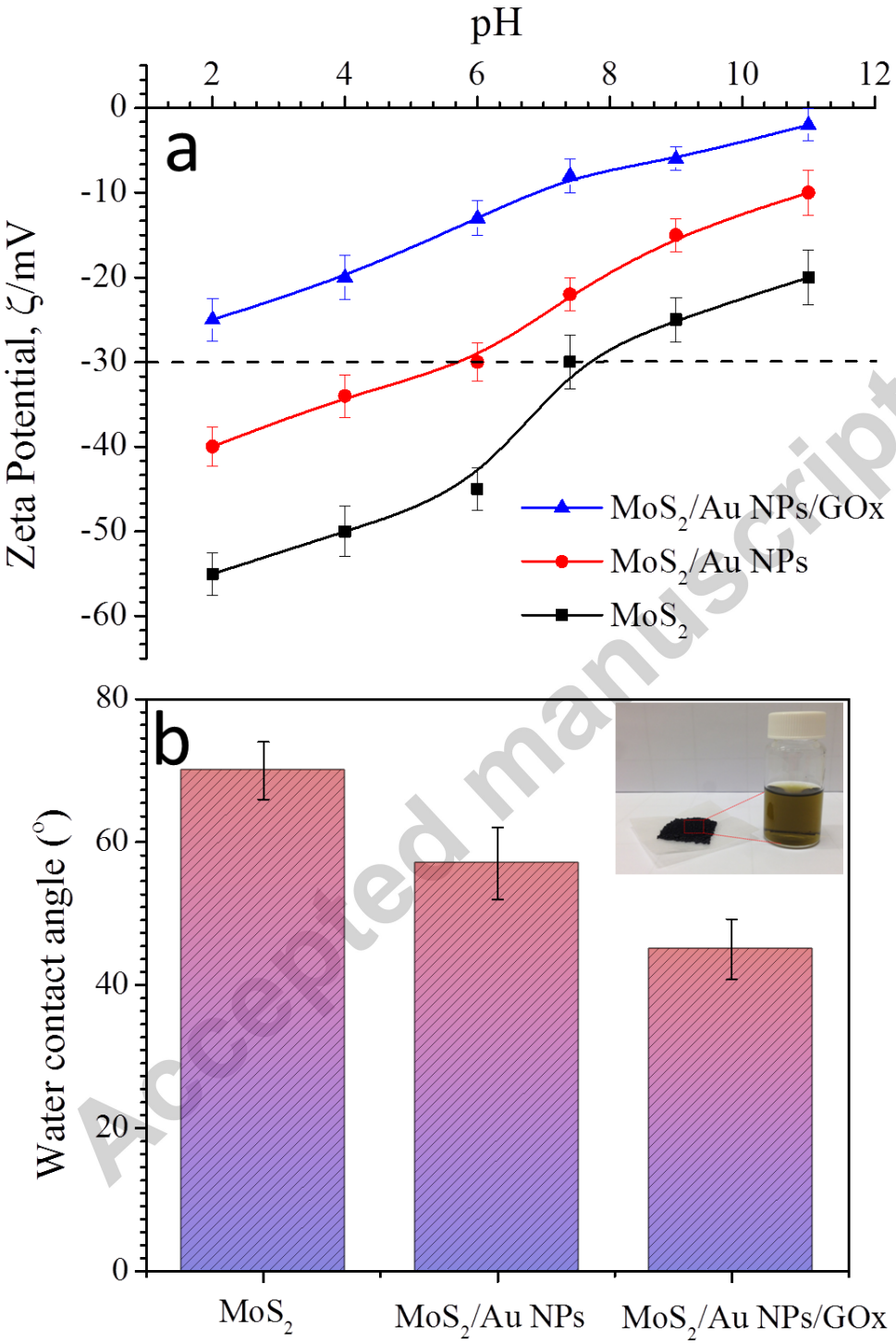

Figure 3. Cyclic voltammetry response of bare and modified gold electrodes in 1 mM ferrocene carboxylic acid and 0.1 M PBS at 50 mV/s vs. Ag/AgCl reference electrode (a), and the effect of scan rates on the cathodic (I_{pc}) and anodic peaks (I_{pa}) of all modified electrodes.

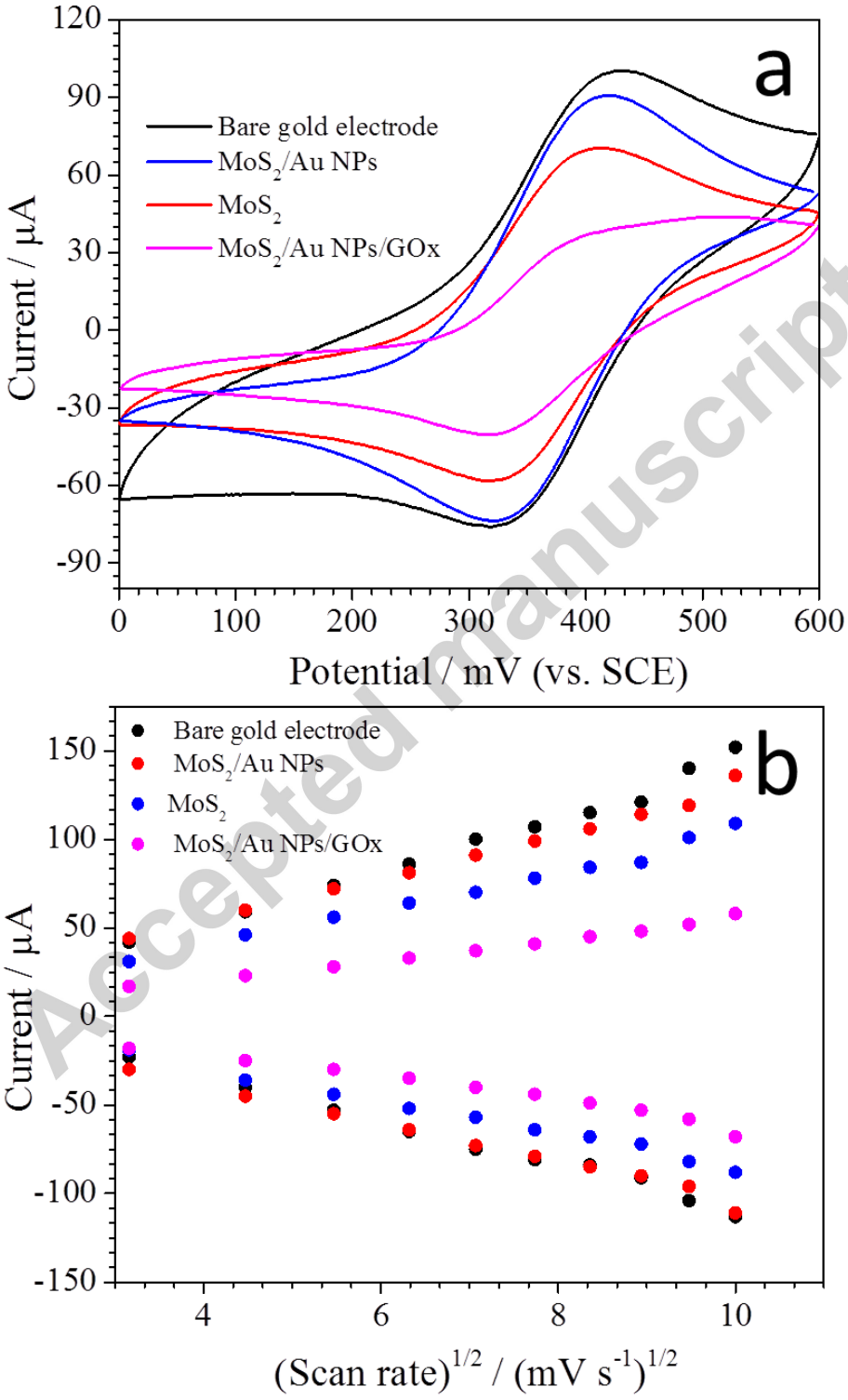

Figure 4. Impedance response of bare and modified electrodes in 1 mM ferrocene carboxylic acid and 0.1 M PBS (a) and histogram for charge transfer resistance (R_{CT}) of all modified electrodes (b).

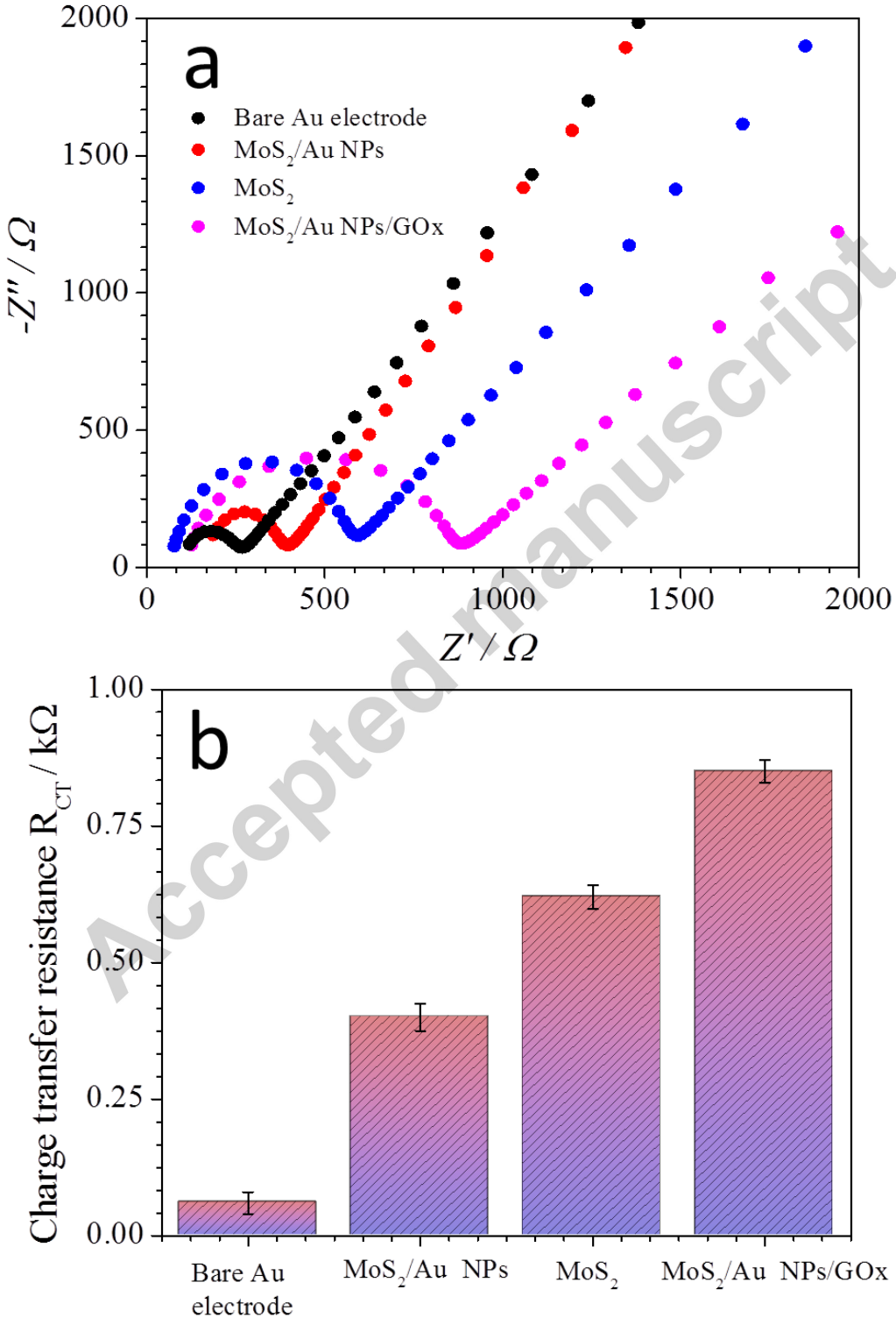

Figure 5. Amperometric responses (a) and calibration curve based on amperometric response for the sensing of glucose with MoS_2/GOx and MoS_2/Au NPs/GOx electrodes in 0.1 M PBS at + 0.35 V applied potential vs. Ag/AgCl.

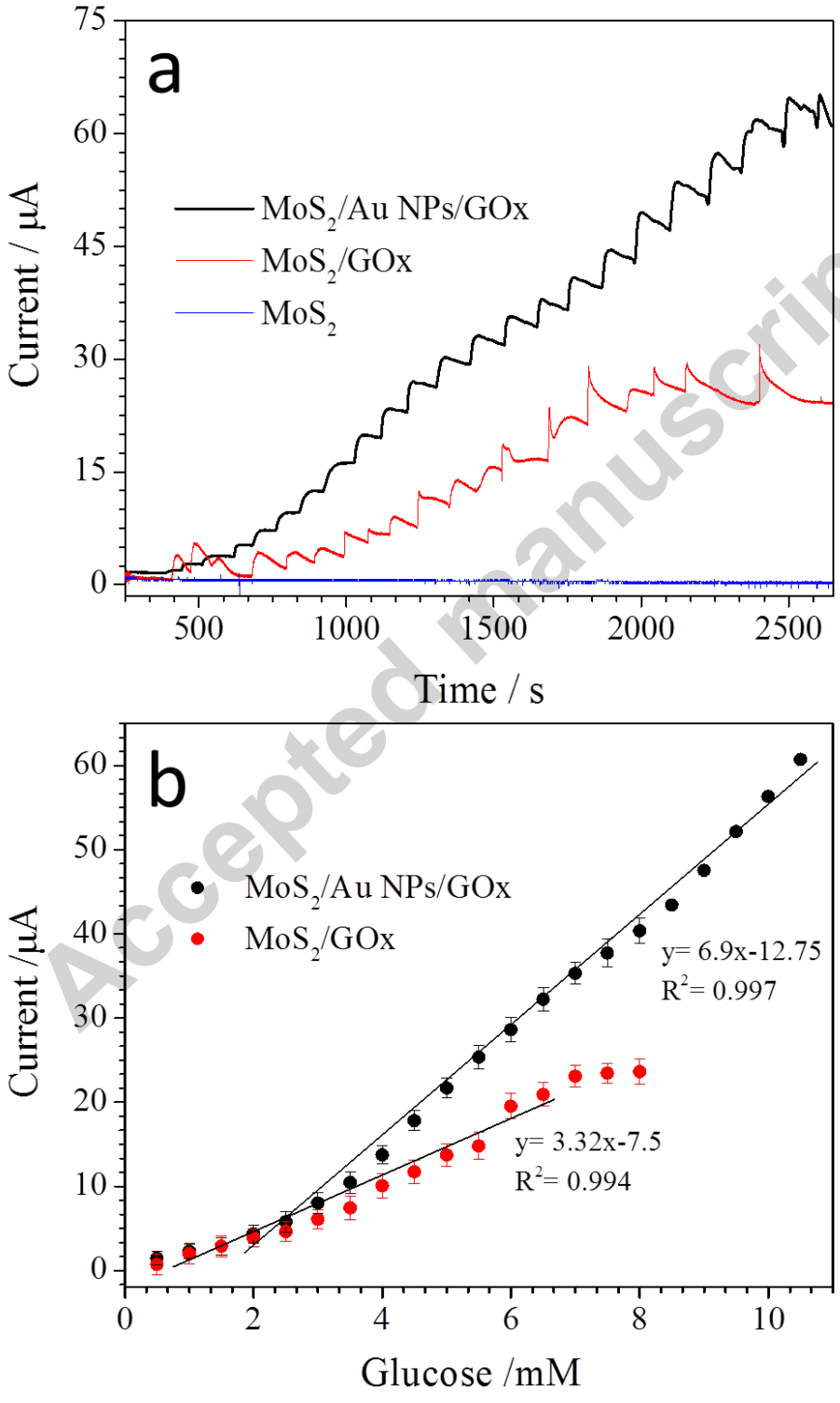

Highlight

- Structuring of gold nanoparticles on two-dimensional molybdenum disulfide (MoS_2) nanosheets in a one-step reaction.
- MoS_2 as a semiconductor, which is an ideal candidate to form homogenous layer on the electrode surface for the structuring of Au NPs.
- The fabrication of an electrochemical biosensor based on MoS_2 nanosheets is demonstrated using a simple, inexpensive and two-dimensional biosystem, which is highly sensitive, selective and stable.
- Design interface could potentially provide significant improvements in biocatalysis and nanotechnology by exploiting this biocatalytic interface with a variety of redox enzymes.